GEOPHYSICS ELECTRICAL CHARACTERIZATION FOR IDENTIFICATION OF SEAWATER INTRUSION IN THE COASTAL AREA OF PAPAR, SABAH

Hardianshah Saleh[1], Siam Jia Quan[2], Muhammad Jaya Padriyamzah Bin Abdul Hamid[3]

[1]Faculty Science and Natural Resources, Universiti Malaysia Sabah.
[2]Faculty of Science and Computer Informatic, Universiti Teknologi PETRONAS.
[3]Wullesdorf Resources Sdn Bhd.

ABSTRACT. *Seawater intrusion is known to be a major problem that influences the quality of groundwater within coastal regions globally. The groundwater table within the coastal area is usually close to the ground surface due to low topography or human development activities such as land reclamation and man-made drainage systems that keep the water table at constant low level. Electrical resistivity method is one of the geophysical methods that has been extensively used to investigate seawater intrusion due to the high electrical conductivity contrast produced by saline water. Papar, Sabah is located at the west coastal region of Sabah and is generally formed by Crocker formation and Quaternary alluvium. The sedimentary rock of Crocker Formation mainly consists of thick sandstone unit, interbedded sandstone, siltstone and shale unit and shale unit. A total of Five 2D electrical resistivity imaging (ERI) methods were carried to image and model the subsurface within the research area to investigate the possibility of seawater intrusion. The ERI results are also supported by four groundwater samples and detailed lithologies from the borehole. Interpretation of the results divided the research area into three main zones of seawater intrusion potentials. Zone 1 is considered the highest potential of seawater intrusion, Zone 2 interpreted as potential extended zone or mixing zones between seawater and fresh water and finally Zone 3 did not indicate any low resistivity or potential of seawater intrusion. The seawater intrusion map produced from this research initiated and divided the potential zones based on the occurrence of seawater in the subsurface.*

KEYWORDS. Geophysics, seawater intrusion, groundwater.

INTRODUCTION

Globally, seawater intrusion is known to be a major problem that influences the groundwater quality within coastal regions globally (Zakiyah Ainul Kamal *et al.,* 2020). The groundwater table within coastal areas is usually close to the ground surface due to low topography or human development activities such as land reclamation and man-made drainage systems that keep water tables at constant

low level (Jiao and Post, 2019; Giambastiani et al., 2020). Generally, the geological and hydrogeological properties of coastal aquifers systems are the key factors in controlling the occurrence and progression of saltwater intrusion (Carrera *et al.,* 2010 and Michael *et al.,* 2013).

External factors such as climate change and human activities also affect groundwater level, especially aquifers in the coastal region (Moser *et al.,* 2014; Green, 2016). Climate change will cause the changing of temperature and precipitation regimes, sea level rise, more frequent extreme weather events and coastal erosion (Norzaida *et al.*, 2017). Changing in temperature and precipitation regimes could have certainly influenced the recharge rate for coastal aquifers and subsequently caused the saltwater intrusion in coastal wells (Griggs, G. & Reguero, 2021). A hot temperature could reduce the amount of rainfall and thus reduce the amount of freshwater input to the aquifer. Furthermore, warmer weather is likely to increase freshwater demand, which may lead to over pumping of the freshwater from aquifers. Combined with sea level rise, this change may bring more frequent and intense storm surges to coastal areas, leading to saltwater flooding around coastal wells (Van Biersal et al., 2007), besides seawater may seep into aquifers from the surface drainage systems. Human activities such as excessive groundwater pumping also contribute to seawater intrusion (e.g., Nawal and Kristine, 2017). This situation results in reducing the hydraulic head in the aquifer, subsequently slowing or stopping the seaward flow of freshwater, which allows seawater to move further inland (Khublalryn *et al.,* 2008).

The Papar coastal area has been developed as the agricultural land to grow plants such as paddy and coconut trees. Since the region is located on the West coast of Sabah, seawater intrusion could become the major threat towards the agricultural industry development which is experienced by many coastal areas in the world (e.g., Lam *et al.*, 2021). Due to the high salt content in the soil, any seawater intrusion within this region would result in a loss of productivity and may make crop cultivation impossible (Tol, 2009). Evaluating and monitoring this situation should become the priority to sustain the groundwater quality as well as agricultural activities (e.g., Lee and Song, 2007).

Geophysical survey for seawater intrusion.

Electrical and electromagnetic techniques have been extensively used in hydrogeological investigations due to the relationship existing between the electrical and hydraulic properties of geological formation and containing fluid saturation (Stewart, 1982; Fitterman & Stewart, 1986; Duque *et al.,* 2008). The electrical resistivity method is one of the geophysical methods that has been extensively used to investigate seawater intrusion due to the high electrical conductivity contrast produced by saline water (e.g, Zakiyah Ainul Kamal *et al.,* 2020; Musta *et al.,* 2022). The technique consists of injecting the electric current into the ground through the electrodes (current electrodes) and measuring the potential difference via other electrodes (potential electrodes) (e.g, Hardianshah & Samsudin, 2016).

Direct quantitative interpretation of apparent electrical conductivity measurements is not easy because it is influenced by several factors, such as porosity, temperature, clay with high cation exchange capacity and concentration of dissolved electrolytes (McNeill, 1980). Thus, the interpretation based on electrical characterization requires in situ data such as geology bore log data

or outcrops observation in the field (e.g., Alajmi *et al.,* 2010).

Hydrogeology parameter of groundwater and salinity.

The pH of groundwater will vary depending on the composition of the rocks and sediments that surround the travel pathway of the recharge water infiltrating the groundwater. Groundwater chemistry will also vary depending on how long the existing groundwater is in contact with a particular rock. Groundwater can be classified based on its physical and chemical properties such as pH, salinity, total dissolved solid (TDS) and electric conductivity (EC). According to Tystsarin (1988) and Miller (2000) the water can be classified to acid sulphate drainage, most natural freshwaters, distilled reverse osmosis water, groundwater, most river water and seawater based on the pH values.

As a basic definition, salinity is the total concentration of all dissolved salts in water (Jain, 2014). Salts form ionic particles as they dissolve, each with a positive and negative charge. Thus, salinity is a strong contributor to conductivity (Hickin, 1995). There are many different dissolved salts that contribute to the salinity of water, the major ions in seawater are chloride, sodium, magnesium, sulfate, calcium, potassium, bicarbonate, bromide, Strontium, Boron and fluoride (Sudaryanto & Wilda, 2017). These ions are also present in inland freshwater such as river water, lake water and pond water but in much smaller amounts. According to Ohrel & Register (2006), the salinity of seawater ranges from 32 ppt to 37 ppt, freshwater is usually lower than 0.5 ppt, and brackish water ranges from 0.5 ppt to 17 ppt. However, the surface salinity of the ocean is more dependent on rainfall, especially areas around the equator and coast where rainfall is high, surface salinity values are lower than average and salinity indicated has a correlation with pH properties (modelled by Radke, 2002).

MATERIALS & METHODS

Investigation of subsurface model and identification of seawater intrusion require geological, geophysics method and hydrogeology input. Thus, this research was conducted by combining several methods and techniques from those fields. All the results were then correlated to produce robust interpretation and understanding regarding the potential of seawater intrusion within the study area.

Geological background of Papar, Sabah.

The Crocker formation dominated the region of West Coast Sabah, which also included the study area within Papar coastal region (**Figure 1**). Papar, Sabah region is generally formed by Crocker formation and Quaternary alluvium (Majeed *et al.,* 1994; Azfar Mohamed *et al.*, 2016). Crocker Formation is used to describe the sedimentary rocks consisting of thick sandstone unit, interbedded sandstone, siltstone and shale unit (Jacobson,1970).

The Crocker Formation of Late Eocene to Early Miocene age is mostly concentrated in the western part of Sabah. The Crocker Formation consists mainly of clastic sediments of flysch type,

which were deposited in an elongated basin of abyssal depth (Collenete, 1958; Jacobson,1970). The sandstone unit is the thickest unit in the Crocker Formation. Individual layer thickness usually exceeds 4 meters and maximum thickness can reach up to 25 meters (**Figure 2a**). It is light grey coloured with grain size medium to coarse, and sometimes pebbly (**Figure 2b**). Interbedded sandstone, siltstone and shale units are defined by an alternating sequence of sandstone, siltstone and shale of variable thickness and ratio. The shale unit is generally composed of grey and red types of shale. The grey variety is occasionally calcareous. It is usually interlayered with siltstone or very fine grain sandstone (**Figure 2c**). While the Quaternary alluvium (**Figure 2d**) is restricted to low land area, coastal areas and riverbank. It mainly consisted of deposited alluvial sediments on river terraces and floodplains and beaches (Majeed *et al.*, 1994).
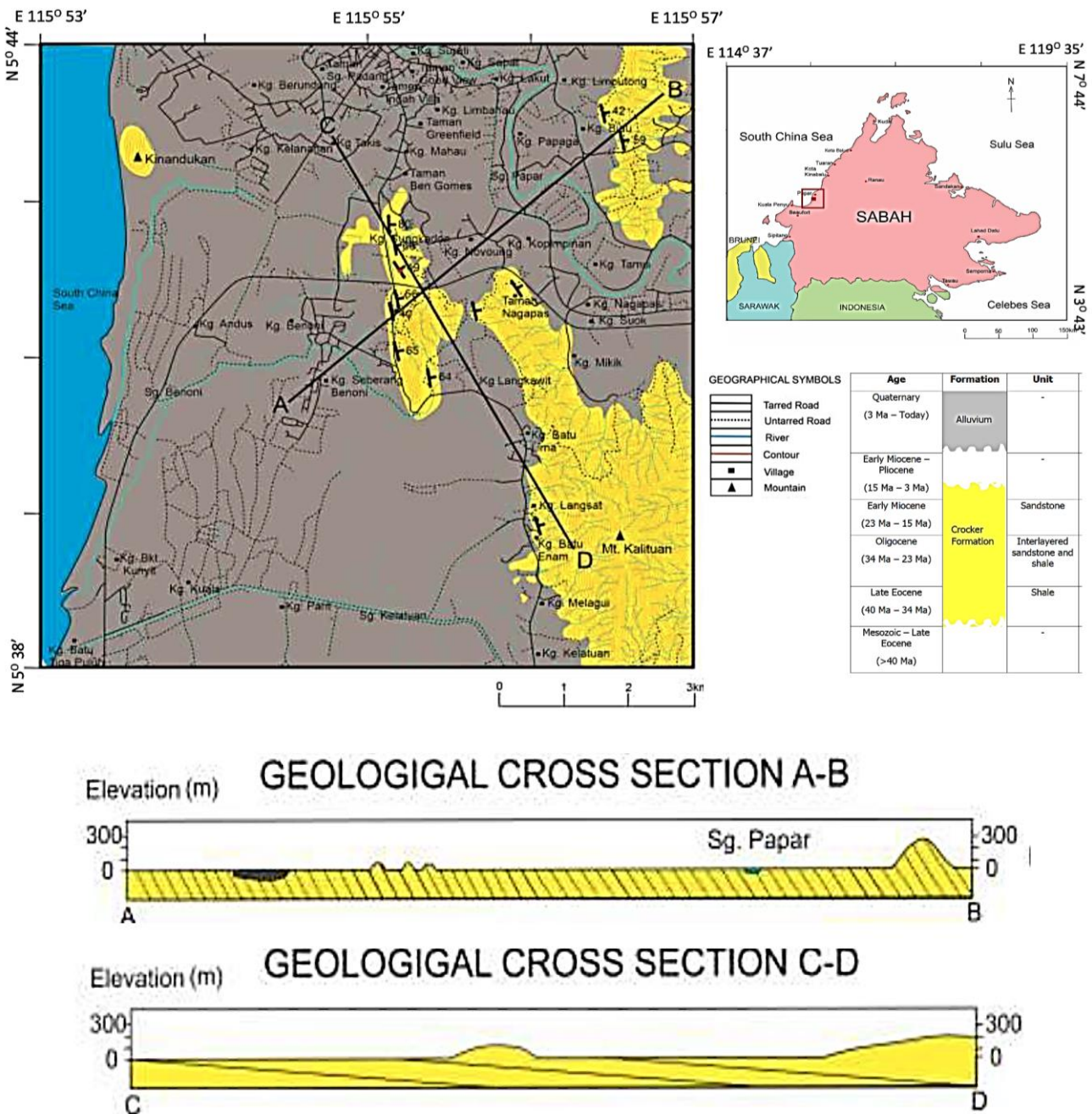

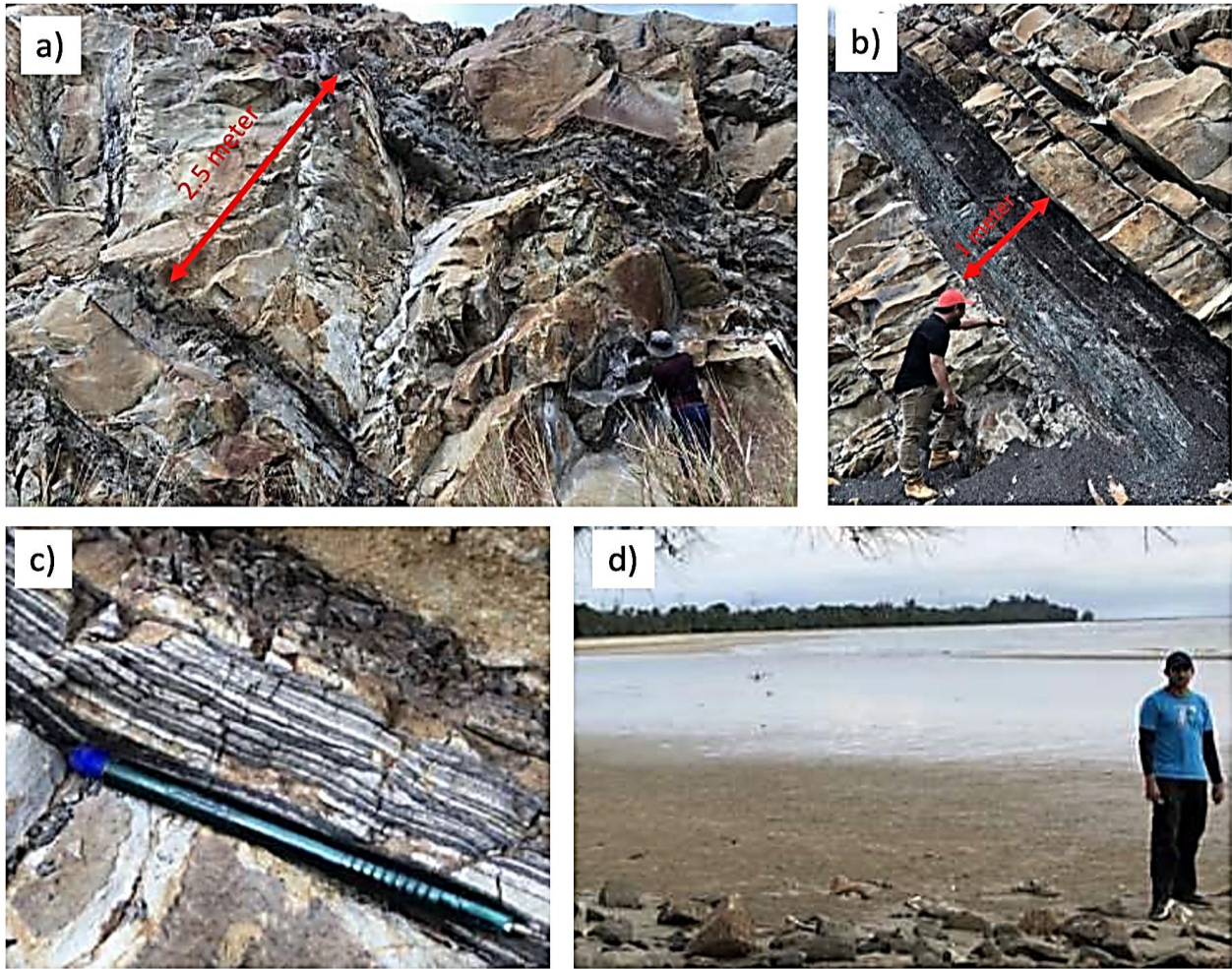**Figure 2. Geological map for the research area.**

Figure 2. Typical Crocker formation and alluvium quaternary within the study area.

Electrical Resistivity Imaging, ERI survey.

Five 2D electrical resistivity imaging (ERI) methods were carried out to image and model the subsurface within the research area to investigate the possibility of seawater intrusion (**Figure 3**). The ERI survey was carried out using ABEM Terrameter LS which connected to stainless steel electrodes with a constant spacing via two or four multicore cables. The ERI survey carried out on all survey points is using 5m electrode spacing which has a total length survey of 200 meters when involving two multicore cables and 400 meters when involving 4 multicore cables. The 200 meters could acquire up to 33 meters of information, while 400 meters gives 80 meters depth of information.

In this studied the Wenner and Schlumberger arrays of electrodes, were used to acquire resistivity data. The Wenner array gives better horizontal resolution, while Schlumberger gives a better depth of information for the same maximum electrode spacing (**Figure 4**). Technically, the Wenner configuration requires 190 data points or resistivity values to model the subsurface. Four electrodes were selected to measure each of these data points, where two electrodes become current electrodes (C1 & C2) to inject current to the ground while another 2 electrodes as potential (PI & P2) to measure electrical potential of the ground. The Schlumberger array using 61 electrodes via four multi-core cables (400 meter) will require 800 of data points. Similarly, two current electrodes (C1 & C2) and two potentials (PI & P2) were used to inject current to the ground and measure current potential. The resistivity values were calculated based on Ohm's Law equation V=IR, resistivity (R)

can be obtained by dividing potential difference (V) to current (I). The resistivity values for subsurface for each datum point are calculated automatically based on the acquisition configuration and stored in the main computer of ABEM Terrameter LS system. The measured resistivity value is then inverted by using RES2DInv to produce a subsurface model (Griffith & Baker, 1993). This 2D subsurface model then correlates with the in-situ data to produce subsurface interpretation for the study area.
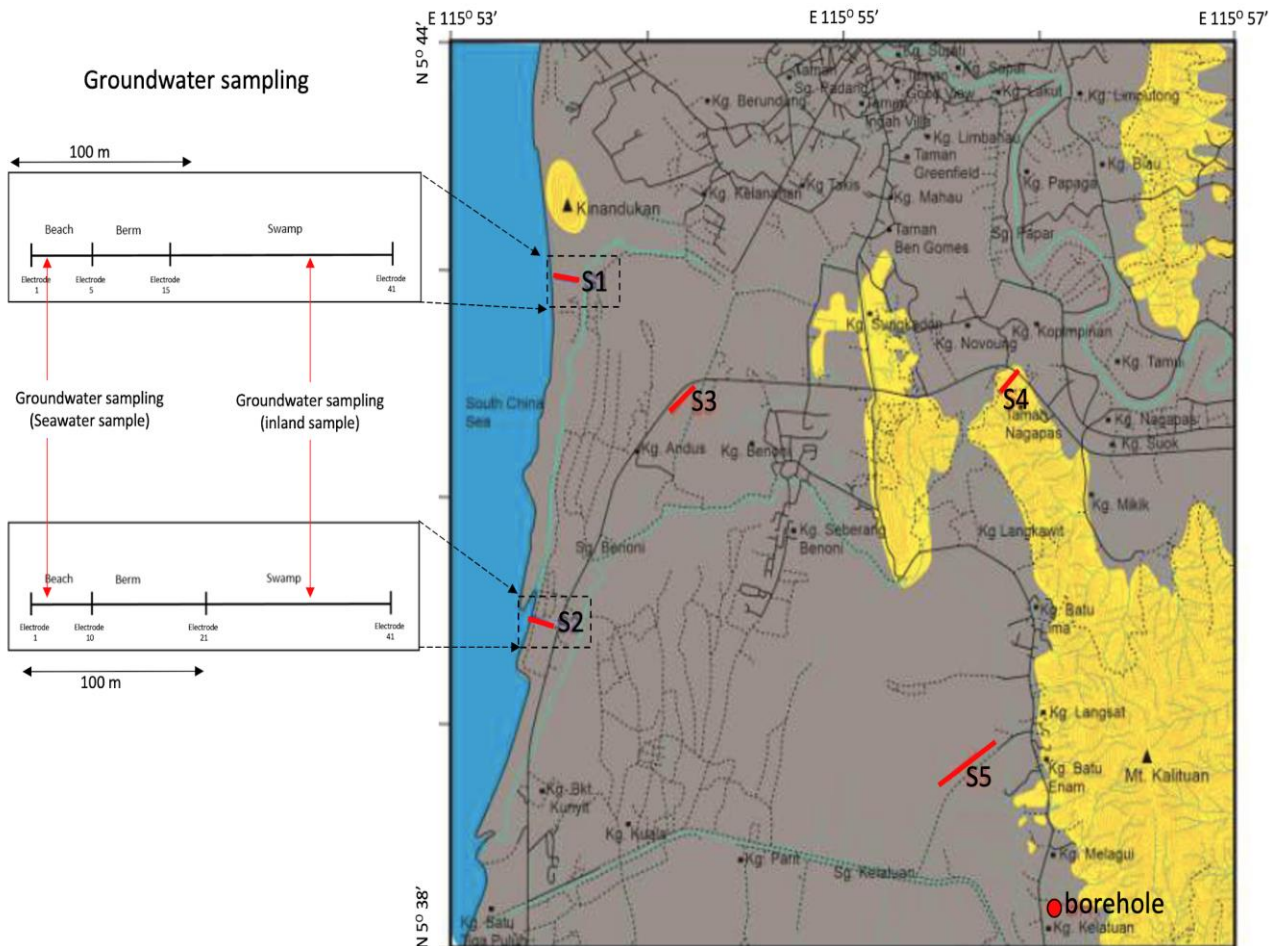

Figure 3. The location of Electrical Resistivity Imaging, ERI survey, groundwater sampling and bore hole.
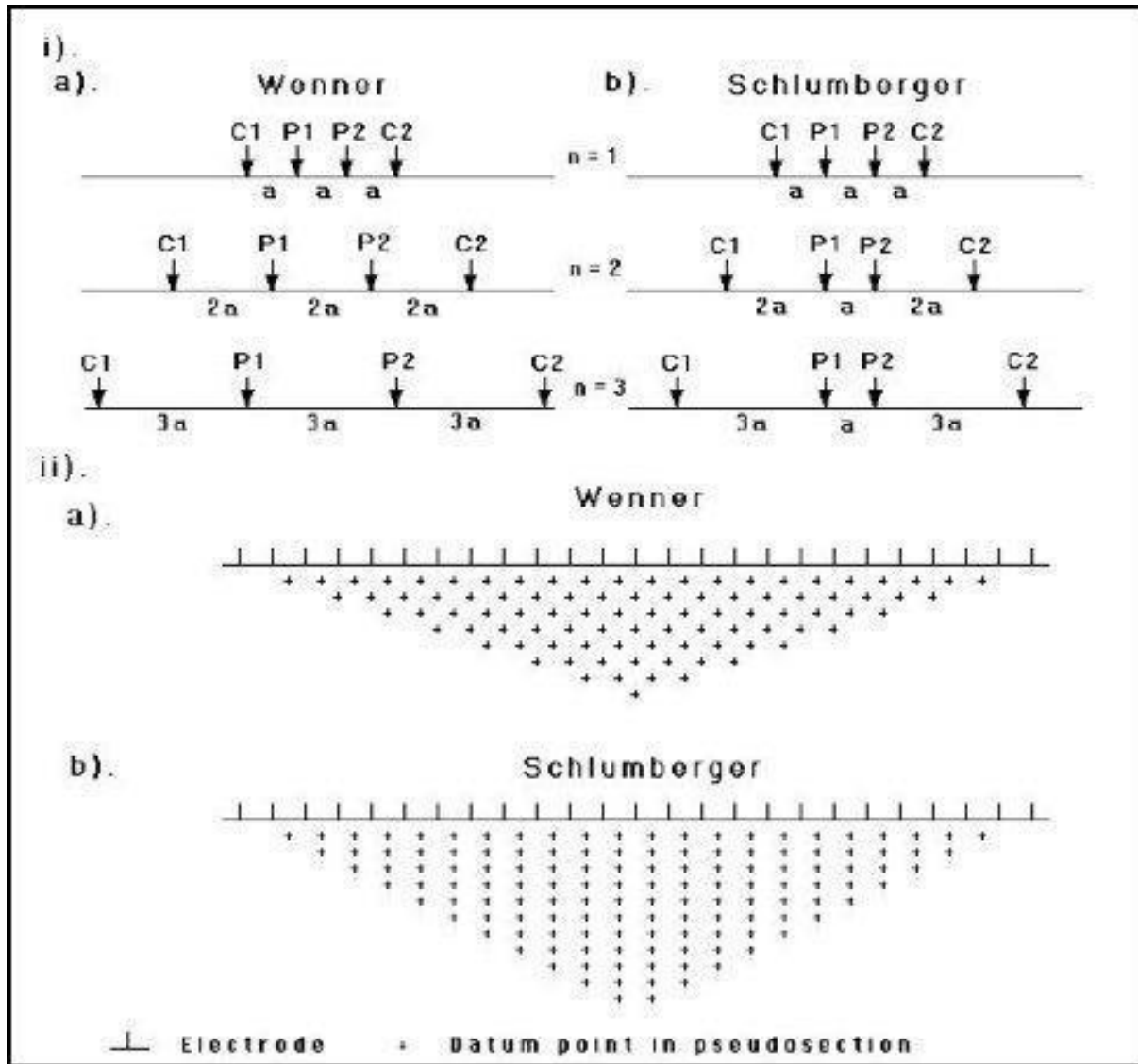
Figure 4. Comparison of ERI data acquisition by using Wenner and Sclumberger configuration (Loke, 1999; Basri *et al.*, 2019)

Physical properties of soil & rock formation.

Borehole data with 79.5 meter of depth (**Table 1**) which is located at Kampung Kelatuan, Papar is used and correlated to interpret the subsurface. It reached depth from 0 meter until 1 meter is unconsolidated fine sand and brown in colour due to high organic matter. From 1 meter until 9.5 meter is consolidated white colour fine sand while for 9.5 meter until 10 meter is consolidated medium grained white colour sand. Next is black shale layer from a depth of 10 meter until 20 meter. At 20 meter to 30 meter depth, there is grey-colored sandstone interlayered with shale or mudstone. At the end, 30 meter until 79.5 meter depth, are shale layers that are dark grey in colour and hard to penetrate. It is interlayered with sandstone layers or other shale layers.

Table 1. Description of subsurface materials from borehole data (Mohd. Kamal, 2011)

Layer	Depth (m)	Lithology
1	0 – 1.0	Unconsolidated brown colour sand
2	1.0 – 9.5	Consolidated white colour fine grained sand
3	9.5 – 10.0	Consolidated white colour medium grained sand
4	10.0 – 20.0	Black shale
5	20.0 – 30.0	Interlayered sandstone and shale unit (sandstone dominated)
6	30.0 – 79.5	Interlayered sandstone and shale unit (mudstone dominated)

Groundwater properties analysis

Two groundwater samples were taken from each of stations S1 and S2 by hand auger (Figure 4). One groundwater sample was taken at the first electrode of the geophysical survey, which is near the shoreface, while the second groundwater sample was collected more inland, which is located between electrodes 30 to 41 or within 150 to 200 meters from the shoreface. Physical properties of the groundwater sample such as pH, salinity, conductivity and total dissolved solid (TDS) were measured in the laboratory by using pH meter and Mettler Toledo Duo pH/ion/conductivity meter.

RESULTS & DISCUSSION

A total of five ERI survey lines with four groundwater analyses were conducted within the research area. Station S1 and S2 have additional groundwater samples from the shoreline and inland to correlate with the ERI results. While stations S5 rely on the borehole data that acquire near this station.

Electrical Resistivity Imaging, ERI results.

The first station is located near the shore face within Telinting Beach. The 200 m of total length survey gave 33.8 m depth of data acquisition. The results indicated that the resistivity value ranged from 0.03 Ωm up to 8 Ωm (**Figure 5a**). While for induced polarization, the chargeability is ranging up to 108.59 msec (**Figure 5b**). Based on ERI results and observation on the field, the subsurface interpreted build up is dominated by unconsolidated sand. The resistivity values are mainly controlled by the salinity and saturation level of seawater since the survey stations were located up to the seashore. Resistivity readings between 0.03 Ωm and 2.73 Ωm are interpreted as fully saltwater saturated sand. For resistivity values range from 5.09 Ωm until 9.47 Ωm which is partially seawater saturated sand for the vadose zone at beach area and low saline water saturated sand at swamp area. For contours with resistivity readings ranging from 17.6 Ωm until 212 Ωm, it is interpreted as sand with different water saturation level. The higher the resistivity the drier the sand.
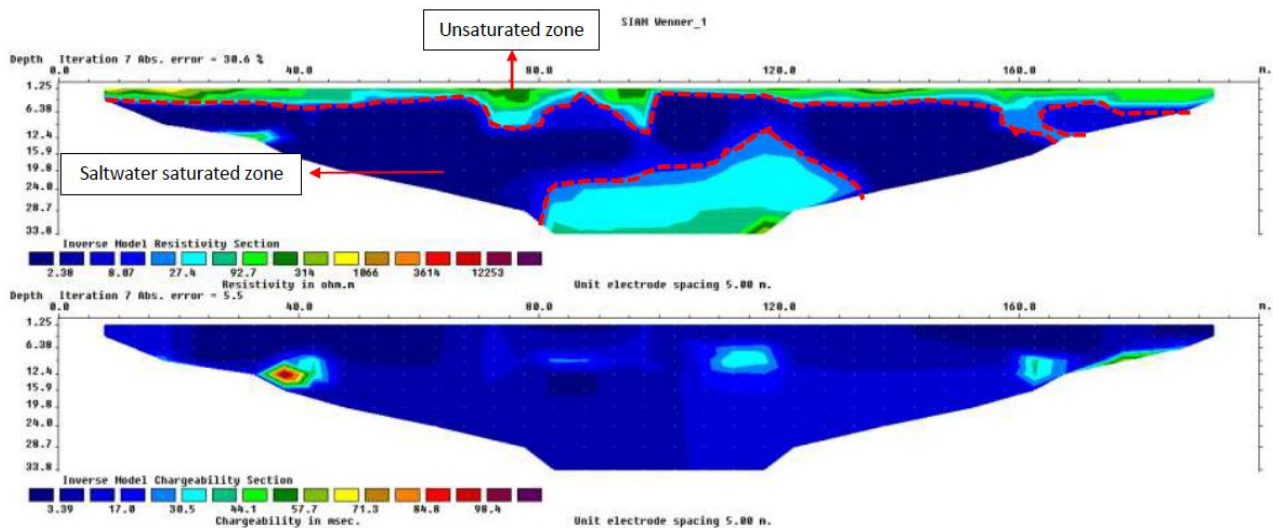
Figure 5. a) Resistivity and b) chargeability value for subsurface of station S1

The ERI results at Station S2 acquired depth of subsurface information up to 33.8 meter from the surface (**Figure 6**). The resistivity reading ranges from 0.18 Ωm up to 247.5 Ωm (**Figure 6a**). While induced polarization indicated the maximum of 49.1 msec (**Figure 6b**). The collected resistivity and induced polarization data are used to correlate with the lab analysis data for subsurface interpretation. The beach area consists of sand particles while swamp areas consist of clay particles (see Lambiase *et al*., 2008). In this area, resistivity readings are mainly controlled by the salinity and saturation level of seawater and soil material. Resistivity readings between 0.22 Ωm and 2.87 Ωm are interpreted as a fully sea water saturated sand layer at the left part of the cross-section. Although the salinity of the water sample collected at the swamp area is low, the resistivity values remain low at the middle right part of the cross-section. This is because soil particles of swamp consist of clay particles with higher cation exchange capacity and high conductivity (Adegoke *et al.,* 2016). This explanation is also supported by the induced polarization cross-section, which shows sudden increase in chargeability values at the right part and indicates the presence of clay layer. For resistivity values range from 4.38 Ωm until 10.2 Ωm is partially seawater saturated sand at the beach area, for contour with resistivity readings range from 15.7 Ωm until 130.9 Ωm is sand with different level of water saturation, the higher the resistivity the drier the sand.
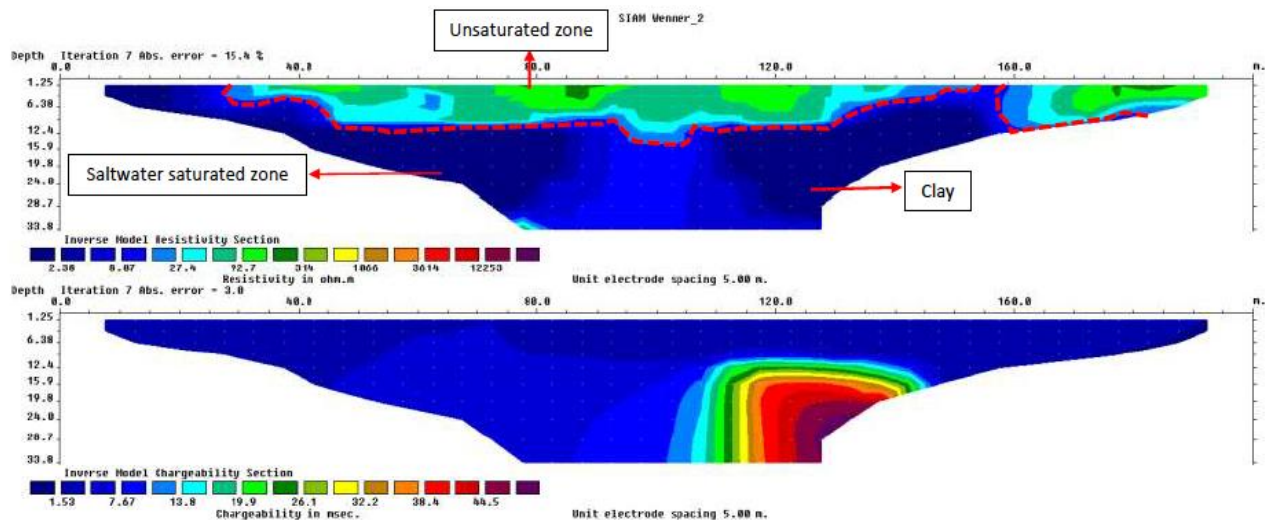

Figure 6. a) Resistivity and b) chargeability value for subsurface of station S2

Station S3 is located at Kampung Benoni, adjacent to a stream. Electrode array used in the electrical resistivity imaging survey for station 3 is Schlumberger array, 4 cable sets with 5 meter electrode distance which makes the total survey line distance is 400 meter with maximum depth of information up to 87.2 meter from the surface. Lowest resistivity reading collected is 0.60 Ωm and the highest is 463.14 Ωm. (**Figure 7**). According to the resistivity cross-section, topsoil consists of sand with different levels of water saturation, the shallower the depth the drier the sand. It has resistivity values ranging from 24.7 Ωm until 463.14 Ωm. Sudden decrease in resistivity around 3 meter depth indicates the level of the water table. Down in the groundwater, the resistivity of water at depth from 12.4 meter until 33.7 meter has relatively lower readings, 0.73 Ωm – 2.36 Ωm and indicates the presence of saltwater (Nassir *et al.,* 2000; Song *et al.,* 2007; Chafouq *et al.,* 2016). Start from depth of 33.7 meter, the resistivity for the saturated zone increased to 3.49 Ωm – 16.7 Ωm indicating salinity level of underground water decrease as depth increases which potentially indicate the appearance of Crocker formation that overlain by the alluvium.
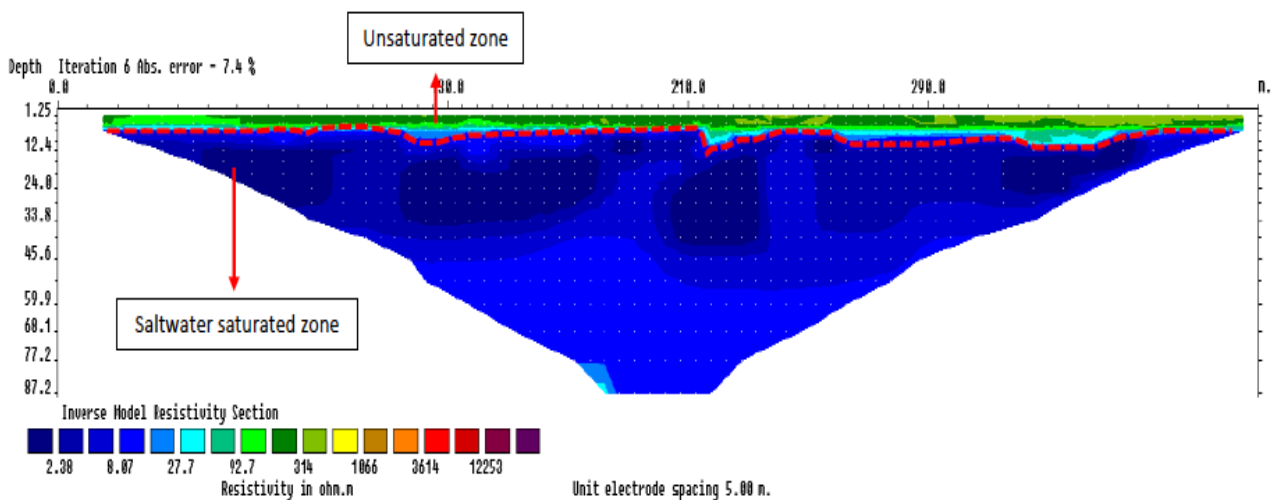

Figure 7. Resistivity (ERT) value for subsurface of station S3

Station S4 is located at Kampung Nagapas with a total distance for survey line is 200 meter with depth of data up to 26.2 meter. Lowest resistivity reading recorded is 1.75 Ωm and the highest is 56370.00 Ωm. An outcrop was found at station 4, it shows interbedded sandstone and shale layers and geological structures such as fault and fold (Majeed Faizal *et al.,* 1995; Lambiase *et al.,* 2008). The resistivity cross-section (**Figure 8**) indicates topsoil of this area reached up to 12.4 meter deep and has lower resistivity value. Resistivity values with the range 1.75 Ωm -14.9 Ωm are interpreted as clayey soil while for resistivity values range from 27.7 Ωm until 314.4 Ωm are known as sandy soil (Hardianshah & Abdul Rahim, 2013). Changing in resistivity horizontally for topsoil indicates weathered interlayered shale and sandstone layers which is the same as the rock layers in the outcrop. Down in the depths, the resistivity values increase, 578.9 Ωm – 56370.0 Ωm as the presence of Crocker Formation bedrock. The lower the weathering grade of the bedrock, the higher the resistivity.
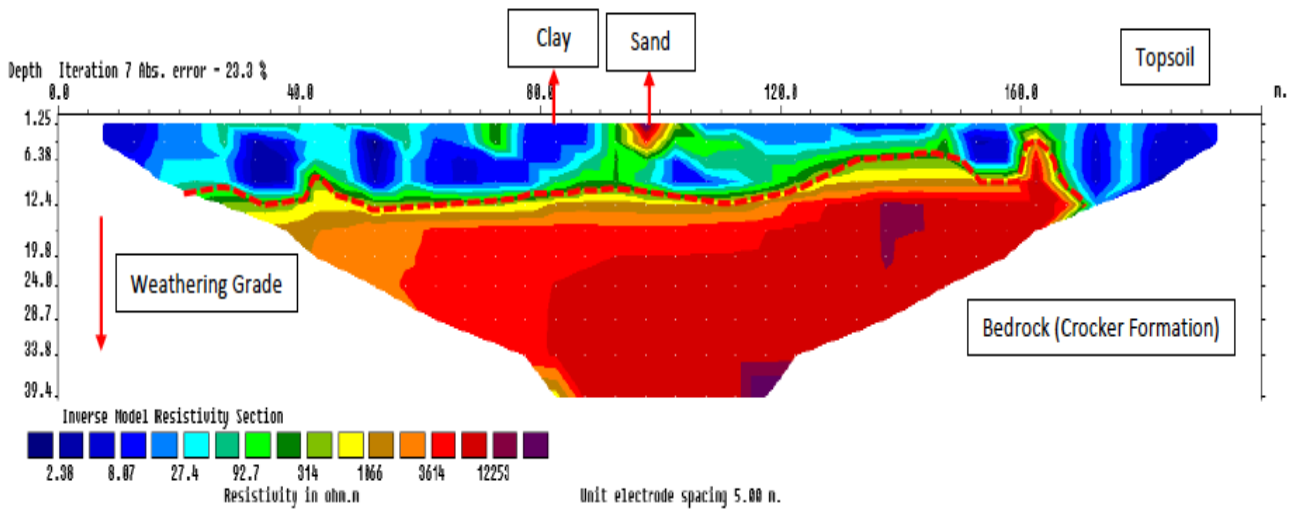
Figure 8. Resistivity (ERT) value for subsurface of station S4

Station S5 located at Kampung Langsat was conducted by using Schlumberger configuration that involved 4 multicore cable which makes the total survey line distance 400 meter. Since the maximum survey line is greater than the previous survey line, ERI results in this station can acquire deeper subsurface information up to 87.2 meter from the surface. The results for station S5 (**Figure 9**) indicate the lowest resistivity reading is 0.09 Ωm and the highest resistivity value up to 1125.90 Ωm.
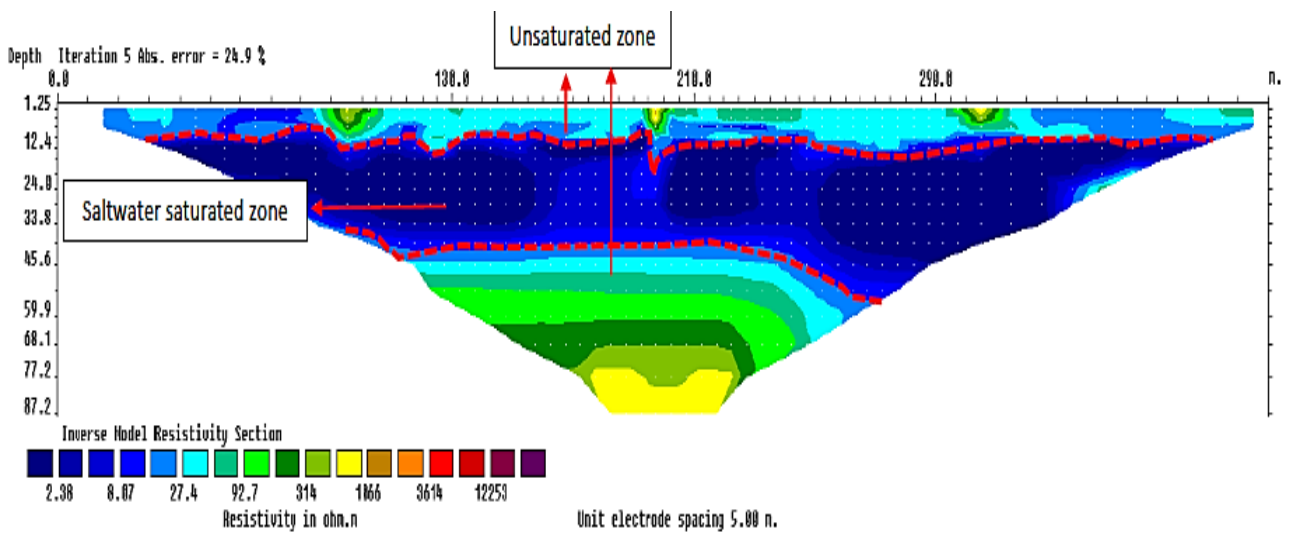

Figure 9. Resistivity (ERT) value for subsurface of station S5

Groundwater analysis from the shoreline region.

Table 2 shows the salinity analysis for water samples collected at stations 1 and 2. The salinity for seawater samples was 28.57 ppt and 16.57 ppt for station 1 and 2 respectively. The salinity values obtained are lower than average due to the rainy season and horizontal stratification of seawater salinity. In horizontal stratification, salinity of seawater increases towards the sea. While for the inland water sample in station S1 indicates the value of salinity is 0.70 ppt. Based on classification

by Ohrel and Register (2006), this water type is categorized as brackish water. Therefore, the area can be categorized as a transition zone between seawater and freshwater and known as saltwater swamp or it was a freshwater swamp originally and intruded by the seawater. The salinity for swamp water collected in station 2 is 0.10 ppt which means the water table zone is free from saltwater pollution.

Table 2. Salinity and pH for groundwater samples at station S1 and S2

Station	Groundwater sample	Average Salinity (ppt)	Average pH
S1	Seawater	28.57	7.73
	Inland	0.7	3.22
S2	Seawater	28.57	7.67
	Inland	0.10	5.04

Table 3. Conductivity for groundwater samples at station S1 and S2

Station	Groundwater sample	Average conductivity (S/cm)
S1	Seawater	0.464
	Inland	1.34×10^{-3}
S2	Seawater	0.027
	Inland	0.21×10^{-3}

The potential of seawater intrusion zones based on geoelectrical characterization.

Based on the interpretation ERI results from five stations (**Table 4**) and water sample analysis, the study area is divided into three main zones of seawater intrusion potentials (**Figure 10**). Zone 1 is considered the highest potential of seawater intrusion as indicated by the ERI results from stations S1 and S2. The appearance of seawater within the subsurface for both stations was confirmed by pH and salinity measured from water samples from these stations.

Table 4. Summary of ERI subsurface interpretation.

Survey Station	Resistivity range (Ωm)	Interpretation	Water table elevation (m)
S1	0.03 – 2.73	Saltwater saturated sand	6.0
	5.09 – 9.47	Brackish water saturated sand	
	17.60 – 999.80	Low saline water saturated sand – dry sand	
S2	0.18 – 2.87	Saltwater saturated sand, saltwater saturated clay	10.0
	4.38 – 10.20	Freshwater saturated clay	
	15.70 – 247.50	Partially freshwater saturated sand – dry sand	
S3	0.60 – 2.36	Saltwater saturated sandstone	10.0
	3.49 – 16.70	Brackish water saturated sandstone	
	24.70 – 463.14	Partially freshwater saturated sand – dry sand	
S4	1.75 – 14.90	Clay	N/A
	27.70 – 324.40	Sand	
	578.90 – 56370.00	Bedrock (Crocker Formation)	

S5	0.09 – 5.92	Saltwater saturated sandstone	12.4
	10.30 – 53.90	Partially saturated mud dominated, Interlayered sandstone and shale unit	
	93.70 – 1125.90	Dry sand, sandstone	

The existence of low resistivity (less than 3 Ωm) extended inland (Zone 2) as indicated and detected within station 3 and 5. This zone is interpreted as a potential extended zone or mixing zones between seawater and freshwater. There are a few parameters that may cause the appearance of low resistivity, such as the existence of clay (Long *et al.,* 2012). The survey area for station S1, S2, S3 and S5 are located within the alluvium which is dominated by clay materials that may cause this low resistivity. Furthermore, based on the resistivity results from stations S1, S2, S3 and S5, the quaternary alluvium deposits within the research area potentially formed an unconfined aquifer system that allow the saline and brackish water to move further inland. Besides, there are many drainages systems (natural and man-made) within the alluvium that may have contributed to this situation. Station S5 is approximately 5.8 km from the coastline, proving saltwater moves far enough inland. Though saltwater is a naturally occurring process, it can also be influenced by human activity in Papar. Overpumping of groundwater for plantation, industry or domestic use can reduce the recharge of fresh groundwater and cause saltwater intrusion. However, saltwater intrusion in Papar due to over-pumping of groundwater has not yet been verified.
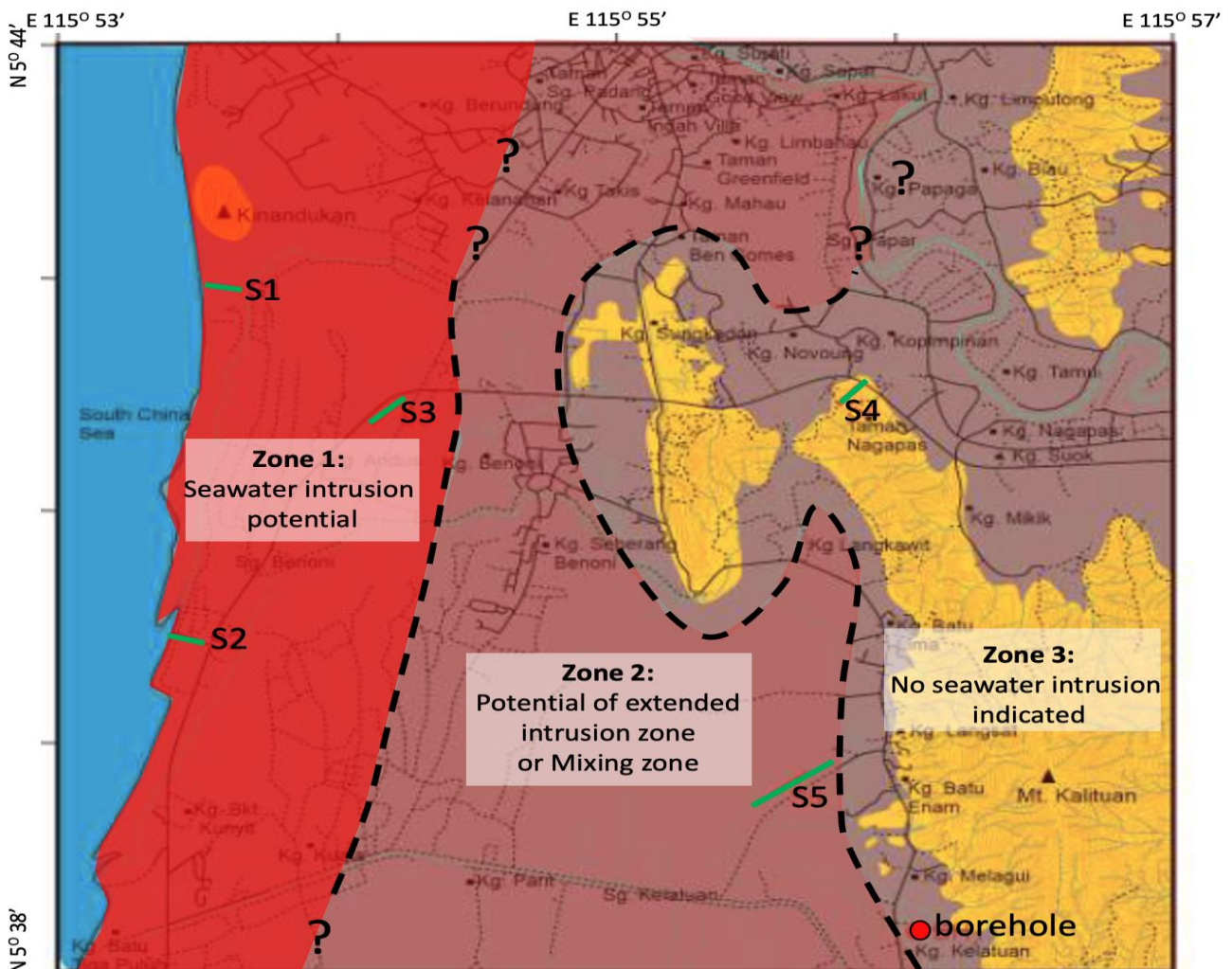

Figure 10. The seawater intrusion potential map.

Station S4 that located on the Crocker formation did not indicate any low resistivity, which also marked as Zone 3 in the Figure 13. The alluvium deposits slightly reach within this zone due to higher topography land (more than 20 m from MSL). This also may suggest that the unconfined aquifer system that build up by the alluvium quaternary did not continuation towards the aquifer system that may formed within the thick sandstone layer in the Crocker formation.

CONCLUSION & SUGGESTION

Correlation of ERI surveys and groundwater analysis gives the subsurface model within the research area. Very low resistivity values ranging from 0.03 Ωm until 6.00 Ωm detected within the subsurface and interpreted as the potential occurrence of seawater intrusion. There are a few parameters that may cause the appearance of low resistivity, such as the existence of clay. The survey area for station S1, S2, S3 and S5 are located within the alluvium which is dominated by clay materials that may cause this low resistivity. This should be able to be justified by using IP data as shown in Station 1 and 2, but unfortunately, due to instrument limitation, IP data is unable to be acquired for Station 3, 4 and 5. Thus, this needs to be confirmed by comprehensive hydro-chemical analysis and to justify whether this low resistivity is influenced by the seawater intrusion itself or the influence of clay mineral from the rock formation or alluvium deposits. Besides, many small channels (natural and man-made) within the alluvium area may transport seawater or brackish water from the shoreline towards the mainland. The subsurface model indicated three apparent zones within the area. Zone 1 indicated the highest potential for seawater intrusion, while Zone 2 indicated mixing zones that also indicated extended potential for seawater intrusion. High topographical areas that are higher than alluvium deposits did not indicate the potential of seawater intrusion.

The seawater intrusion map produced from this research initiated and divided the potential zones based on the occurrence of seawater in the subsurface. While some improvements need to be made to produce robust and detailed mapping such as additional the numbers of ERI survey lines and monitoring well among the proposed zones. This will provide a better image or idea of the condition of seawater intrusion and identify the absolute border between seawater, freshwater and mixing zone precisely.

ACKNOWLEDGEMENT

REFERENCE

Adegoke, J.A., Egbeyele, G. & Akinyemi, O.D. 2016. Effect of CEC of clay on thermal conductivity. *Malaysian Journal of Science*, Vol. 35 (2), Pp. 107-116.

Al-Ajmi, Hussain & Hinderer, Matthias & Keller, Martin & Rausch, Randolf & Blum, Philipp & Bohnsack, Daniel. 2010. The Role of Outcrop Analogue Studies for the Characterization of Aquifer Properties. *International Journal of Water Resources and Arid Environments.* **1(1)**: 48-54, 2011ISSN 2079-7079

Azfar Mohamed, Abdul Hadi Abd Rahman & Mohd Suhaili Ismail. 2016. Sedimentary Facies of the West Crocker Formation North Kota Kinabalu-Tuaran Area, Sabah, Malaysia. *IOP Conf. Ser.: Earth Environ. Sci.* **30** 012004

Basri, Kasbi & Wahab, Norhaliza & Abu Talib, Mohd Khaidir & Zainorabidin, Adnan. (2019). Sub-surface Profiling Using Electrical Resistivity Tomography (ERT) with Complement from Peat Sampler. *Civil Engineering and Architecture*. **7**. 7-18. 10.13189/cea.2019.071402.

Chafouq, D.; Mandour, A.E.; Elgettafi, M.; Himi, M.; Bengamra, S.; Lagfid, Y.; Casas, A. 2016. Assessing of saltwater intrusion in Ghiz-Nekor aquifer (North Morocco) using electrical resistivity tomography. *Near Surf. Geosci*, Pp.1–6

Carrera, J., Hidalgo, J. J., Slooten, L. J., & V zquez-Su, E. 2010. Computational and conceptual issues in the calibration of seawater intrusion models. *Hydrogeology Journal*, **18**: 131-145.

Collenette, P. 1958. *The Geology and Mineral Resources of the Jesselton- Kota Kinabalu Area, North Borneo*. W.J.Chater, Government Printer.

Duque, C., Calvache, M. L., Pedrera, A., Rosalees, W. M. & Chicano, M.L. 2008. Combined time domain electromagnetic soundings and gravimetry to determine marine intrusion in a detrital coastal aquifer (Southern Spain). *Journal of Hydrology*, 536-547.

EPA. 2014. Sediments. In Water: Pollution Prevention & Control. Retrieved from http://water.epa.gov/polwaste/sediments/).

Fitterman, D.V., Stewart. M.T. 1986. Transient electromagnetic sounding for groundwater. *Geophysics*, **51(4)**: 995-1005.

Giambastiani BMS, Macciocca VR, Molducci M, Antonellini M. Factors Affecting Water Drainage Long-Time Series in the Salinized Low-Lying Coastal Area of Ravenna (Italy). Water. 2020; 12(1):256. https://doi.org/10.3390/w12010256.

Green T.R. 2016. Linking Climate Change and Groundwater. In: Jakeman A.J., Barreteau O., Hunt R.J., Rinaudo JD., Ross A. (eds) *Integrated Groundwater Management*.

Griffiths, D. and R. Barker, 1993. Two-dimensional resistivity imaging and modelling in areas of complex geology. *Journal of applied Geophysics,* 1993. 29(3-4): p. 211-226.

Griggs, G. & Reguero, B.G. 2021. Coastal Adaptation to Climate Change and Sea-Level Rise. *Water*, **13**, 2151. https://doi.org/10.3390/w13162151

Hardianshah, S. & Abdul Rahim, S. 2013. Geo-electrical resistivity characterization of sedimentary rocks in dent peninsular, lahad datu, sabah. *Borneo Science*, **32**.

Hickin, E. J. (Ed.). 1995. *River Geomorphology*. Chichester: Wiley.

Jacobson, G. 1970. Gunong Kinabalu area, Sabah, Malaysia. *Geological Survey Malaysia. Report 8*.

Jain C.K. 2011. Salinity. In: Singh V.P., Singh P., Haritashya U.K. (eds) *Encyclopedia of Snow, Ice and Glaciers. Encyclopedia of Earth Sciences Series*. Springer, Dordrecht. https://doi.org/10.1007/978-90-481-2642-2_461.

Jiao, J., & Post, V. 2019. Impact of Land Reclamation on Coastal Groundwater Systems. In *Coastal Hydrogeology* (pp. 255-282). Cambridge: Cambridge University Press. doi:10.1017/9781139344142.009.

Kanagaraj G, Elango L, Sridhar SGD and Gowrisankar G. 2018. *Environmental Science and Pollution Research*, **25**. 8989.

Khublaryan, M.G., A.P. Frolov, and I.O. Yushmanov. 2008. Seawater intrusion into coastal aquifers. *Water Resources*, **35(3)**: 274–86.

Lam, Y., Winch, P.J., Nizame, F.A. Broaduss-Shea, E.T., Harun, M.G.D & Surkan, P.J. 2021. Salinity and food security in southwest coastal Bangladesh: impacts on household food production and strategies for adaptation. *Food Sec*, **2021**. https://doi.org/10.1007/s12571-021-01177-5.

Lambiase, J.J., Tzong, T.Y., William, A.G., Bidgood, M.D., Brenac, P., and Cullen, A.B., 2008, The West Crocker formation of northwest Borneo: A Paleogene accretionary prism, *ln* Draut, A.E., Clift, p.D., und Scholl, D.W., eds., Formation and Applications of the Sedimentary Record in Arc Collision Zones: *Geological Society of America Special* paper 436, p. l7 l-184, doi: 1 0.1 1 30/2008.2436(08).

Lee, Jin-Yong & Song, Sung-Ho. 2007. Evaluation of groundwater quality in coastal areas: Implications for sustainable agriculture. *Environmental Geology*. **52**. 1231-1242. 10.1007/s00254-006-0560-2.

Loke, M., 1992. *Electrical imaging surveys for environmental and engineering studies. A practical guide to 2-D and 3-D surveys*.

Long, M., Donohue, S., L'Heureux, J-S., Solberg, I-L., Rønning, J-S, Limacher, R., O'Connor, P., Sauvin, G., Rømoen, M. and Lecomte, I. 2012. Relationship between electrical resistivity and basic geotechnical parameters for marine clays. *Canada Geotech. J.* Vol. 49, Pp.1–11.

Majeed Faisal, Shariff A.K. Omang & Sanudin HJ. Tahir. 1994. Geology of Kota Kinabalu and its implications to groundwater potential. *Bulletin Geol. Soc. Malaysia*, **38**, 11-20.

McNeill J. D. 1980. *Survey Interpretation Techniques*. Geonics, Ltd., Misissauga, Canada, Technical Note TN-5.

Michael, H. A., Russoniello, C. J., & Byron, L. A. 2013. Global assessment of vulnerability to sea-level rise in topography-limited and recharge-limited coastal groundwater systems. *Water Resources Research*, **49**: 2228-2240.

Miller, G.T. 2000. Living in the Environment, Brooks/Cole Publishing Company, Pacific Grove. Haines, Skyring, Stephens, Papworth (2001) Managing Lake Wollumboola's Odour Problem. Proc. 11th NSW Coastal Conference, Newcastle 13-16 November 2001.

Mohd. Kamal. 2011. Kimanis power plant field subsurface exploration log. STL Geotechnical Engineering Sdn. Bhd. Unpublished report.

Moser, S. C., M. A. Davidson, P. Kirshen, P. Mulvaney, J. F. Murley, J. E. Neumann, L. Petes, and D. Reed, 2014: Ch. 25: Coastal Zone Development and Ecosystems. Climate Change Impacts in the United States: The Third National Climate As-sessment, J. M. Melillo, Terese (T.C.) Richmond, and G. W. Yohe, Eds., U.S. Global Change Research Program,579-618. Springer,Cham.

Musta, B., Asat, M.A., Ling, S.Y. & Saleh, H. 2022. Geophysical Investigation and Geochemical Study of Sediment along the Coastal Area in Kota Belud Sabah, Malaysia. *Journal of Physics: Conference Series*, **2165 (1).**

Nawal Alfarrah and Kristine Walraevens, 2017. Groundwater Overexploitation and Seawater Intrusion in Coastal Areas of Arid and Semi-Arid Regions. *Water*, **10**, 143; doi:10.3390/w10020143.

Nassir, A.S.S. Loke, M.H. Lee, C.Y & Nawawi, M.N.M. 2000. Salt-water intrusion mapping by geoelectrical imaging surveys. *Geophys. Prospect*, Vol. 48, 647–661.

Norzaida Abas, Zalina Mohd Daud, Norazizi Mohamed & Syafrina Abdul Halim, 2017. Climate change impact on coastal communities in Malaysia. *Journal of Advanced Research Design*. **33**. 1-7.

Ohrel, R. and Register, K. 2006. *Volunteer Estuary Monitoring: A Methods Manual*. U.S. Environmental Protection Agency (EPA), Office of Wetlands, Oceans and Watersheds, The Ocean Conservancy.

Radke, L.C. 2002. Water allocation and critical flows: potential ionic impacts on estuarine organisms. *Proceedings of Coast to Coast 2002 – "Source to Sea",* Tweed Heads, pp. 367-370.

Song, S.H.; Lee, J.Y.; Park, N. 2007. Use of vertical electrical soundings to delineate seawater intrusion in a coastal area of Byunsan, *Korea. Environ. Geol*, Vol. 52, Pp. 1207–1219

Stewart. M.T. 1982. Evaluation of Electromagnetic Methods for Rapid Mapping of Salt-Water Interfaces in Coastal Aquifers. *Groundwater*, **20 (5)**: 538-545.

Sudaryanto and Wilda Naily. 2018. Ratio of Major Ions in Groundwater to Determine Saltwater Intrusion in Coastal Areas. *IOP Conf. Ser.: Earth Environ. Sci.* **118** 012021.

Tol, R.S.J. 2009. Economics of Sea Level Rise, Editor(s): John H. Steele, Encyclopedia of Ocean Sciences (Second Edition), Academic Press, Pages 197-200, ISBN 9780123744739, https://doi.org/10.1016/B978-012374473-9.00774-8.

Van Biersel, T.P., D.A. Carlson, and L.R. Milner. 2007. Impact of hurricane storm surges on the groundwater resources. *Environ Geol*, 53: 813–26.

Zakiyah Ainul Kamal, Mohd Syakir Sulaiman, Muhammad Khairul Hakim, Thilageswaran, Anis Syahira, Zahidi Hamzah and Mohammad Muqtada Ali Khan. 2020. Investigation of Seawater Intrusion in Coastal Aquifers of Kelantan, Malaysia using Geophysical and Hydrochemical Techniques. *IOP Conf. Ser.: Earth Environ. Sci*. 549 012018.